DSI3 Sensor to Master Current Threshold Adaptation for Pattern Recognition

David Levy
Infineon Austria AG, Automotive Power Train Systems, Villach, Austria
Email: david.levy@infineon.com

***Abstract*—The newly released Distributed System Interface 3 (DSI3) Bus Standard specification defines 3 modulation levels form which 16 valid symbols are coded. This complex structure is best decoded with symbol pattern recognition. In order to simplify the pattern recognition correlation calculation, the received differential current is quantized back to 3 levels. This paper describes how the thresholds are estimated and adapted for the most optimum quantization. The complete system was simulated in Matlab script. It will be shown that after 24 symbols, the estimated threshold is 6% away from the optimum thresholds when the initial currents are 35% off the expected nominal thresholds. This proves fast convergence to the optimal threshold and a small residual error in a system that includes the major distortions and inaccuracies.**

***Index Terms*—automotive, DSI3, symbol decoding, threshold estimation, threshold adaptation**

I. Introduction

DSI3 Bus Standard specification [1] is promoted by the DSI consortium. DSI3 goals are to improve performance, reduce cost and promote open standard. Higher performance is achieved among others, by increased communication speed from the slave sensor to the master. The higher communication speed is achieved by compressed bit encoding.

Each incoming sample current is quantized to 3 levels, based on an adapting threshold. The quantized levels are then input to a correlation machine. Thanks to the quantization, the correlation machine can be kept very simple. The correlation mechanism is described in another paper. This paper describes a method to adapt the threshold to the optimum threshold.

The performance of the proposed method is checked with a Matlab simulation. The simulation includes the complete system: sensor, harness and decoder. Depending on the load models the threshold estimation manages to reach an error below 6\% from the optimum threshold in 24 symbols when starting with an error of 35\%.

The organization of the paper is as follow: section II describes the DSI3 bit decoding. Section III describes existing threshold adaptation mechanisms. Section IV defines the proposed adaptation mechanism. Section V shows the performance achieved with the proposed method. Section VI summarizes the paper.

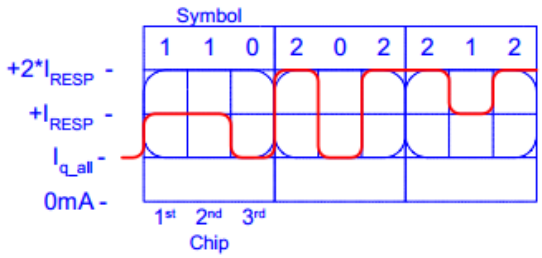

Figure 1. Coding example.

II. Background

The sensor slave encodes response frames to the master with current modulation. The master supplies the slaves with a quiescent current. The slave modulates this current in a way that the master has to supply a higher current during data modulation. The DSI3 standard defines three current modulation levels:

- 0: this current level is identical to the quiescent current supplied by the master
- 1: this current level is I_{RESP} above the quiescent current
- 2: this current level is $2I_{RESP}$ above the quiescent current

The smallest chunk of information is called chip, which represents one current level. The minimum duration during which the slave keeps the modulated current at the same level during data transmission is t_{chip}.

Three chips are combined to form a symbol. The slave encodes 4 bits of data in a symbol. An example of such a coding is given in Fig. 1 and the complete coding table is given in Table I.

III. Prior Art

The PSI5 standard [2] uses Manchester encoded current modulation for sensor data transfer to the main unit. The Manchester encoding has two levels and two chips per symbol. The two possible symbols are symmetric. The advantage of these properties is that whatever data is transferred, the threshold between the two levels is always simply the average current during the frame.

Manuscript received July 16, 2013; revised November 14, 2013

doi: 10.12720/ijsps.1.2.141-145

TABLE I. DATA TO SYMBOL MAPPING

Data	1st chip	2nd chip	3rd chip
0	1	1	0
1	2	1	1
2	1	0	2
3	2	0	2
4	1	0	0
5	2	1	2
6	1	1	2
7	2	0	1
8	2	2	0
9	2	1	0
10	1	2	2
11	2	2	1
12	1	2	0
13	2	0	0
14	1	0	1
15	1	2	1

The adaptive quantizer, proposed by Jayant [3], adapts its step size by a factor depending on the knowledge of which quantizer slot was occupied by the previous signal sample. Unfortunately the choice of this multiplication factor depends on the input signal type. Jayant considered Gauss-Markov inputs with different correlation factors from one sample to the next and derived the optimum multiplication factors for these types of inputs. The DSI3 case is unfortunately not a Gauss-Markov signal, and therefore, it would require an extensive set of simulations to find the optimum multiplication factors.

In references [4] and [5], it is assumed the input data to be Gaussian. The DSI3 statistics would show a trimodal distribution, because the current has a much higher probability to be close to one of the three allowed current levels. The methods for adaptive quantization proposed cannot be used for DSI3 current modulation decoding.

In reference [6], Ortega proposes an adaptive quantizer that estimates the input probability function distribution (pdf). Based on this function, it tunes the quantizer parameters optimally and computes the next time the pdf has to be re-estimated. The pdf estimation consists in assuming that the probability that a sample is greater than the highest quantization level or smaller than the lowest one is zero. Unfortunately this assumption is impossible for a two-level only quantizer, which is our case.

Reference [7], a Wireless sensor dedicated adaptive quantization is proposed. It requires running the Variational algorithm and calculating the Fisher Information matrix for every sample. These complex operations are not suitable for DSI3 where the chip duration can be as low as 2.75 µs.

Reference [8], adaptive quantization for signals of Gaussian mixture model (GMM) is proposed. This would fit best to the DSI3 because the trimodal distribution is a GMM with three Gaussian components. The authors focus on the simple GMM which consists of two components, but also describe the extension to a general GMM. The first step consists in finding the mean and variance of each Gaussian component, using the expectation-maximization (EM) algorithm. Unfortunately, the EM algorithm, described in reference [9], is much too complex to implement in hardware on signals sampled an order of magnitude faster than $1/t_{chip}$ rate.

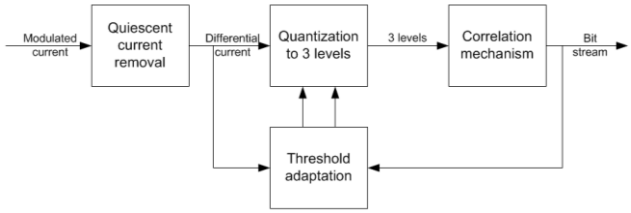

Figure 2. Block Diagram.

IV. THRESHOLD ADAPTATION ALGORITHM

The receiver has to remove the quiescent current and to quantize the current levels. The quiescent current is removed by an estimation of the DC current when no data modulation takes place. The quantization is achieved by comparing to thresholds. One threshold is for differentiating between level 0 (corresponding to the quiescent current) and level 1 (corresponding to I_{RESP} above the quiescent current). The other threshold is for differentiating between level 1 and level 2 (corresponding to $2I_{RESP}$ above the quiescent current). The values of those thresholds have to be estimated and continuously adapted. The quantized samples are used by the correlation machine which recognizes expected patterns. Thanks to the quantization, the correlation machine only needs to memorize 2 bits per sample instead of the complete current, and the correlation is a simple comparison rather than the theoretical multiplication. The block diagram is shown in Fig. 2. The correlation mechanism is detailed in a separate paper.

The algorithm outputs a set of threshold estimations for each symbol detected by the correlation mechanism. The beginning of the first symbol in the frame is the first time the differential current level 1 threshold is crossed. The beginning of the subsequent symbols is detected by the correlation mechanism.

The average measured current for the duration of the symbol, μ_m, is given in (1),

$$\mu_m = \frac{1}{n_s}\sum_{i=1}^{n_s} I_m[i] \tag{1}$$

where n_s is the number of current samples in the detected symbol and $I_m[i]$ is the measured differential current of sample i. n_s may vary from symbol to symbol due to channel phase distortion or clock mismatch between sensor and master.

As can be seen from Table I, the average current varies per symbol. Therefore, the recognized symbol, received

from the correlation mechanism must be used to calculate the expected current. The expected average current, μ_e, is given in (2),

$$\mu_e = \frac{1}{3}(n_{c1}I_1[s-1] + n_{c2}I_2[s-1]) \tag{2}$$

where n_{c1} and n_{c2} are the number of chips at level 1 and 2, respectively, for the recognized symbol. For example, for data 1 (second line in Table I), n_{c1}=2 and n_{c2}=1. $I_1[s-1]$ and $I_2[s-1]$ are the previous symbol calculated differential currents for for level 1 and level 2 respectively.

The error, ε, is simply the difference between the measured and expected current.

$$\varepsilon = \mu_m - \mu_e \tag{3}$$

The error can also be split to error on level 1, ε_1, and error on level 2, ε_2, as shown in (4).

$$\varepsilon = \frac{1}{3}(n_{c1}\varepsilon_1 + n_{c2}\varepsilon_2) \tag{4}$$

Assuming that there is no saturation effect on the currents for the range considered, we have:

$$I_1[s] = \frac{I_2[s]}{2} \tag{5}$$

$$\varepsilon_1 = \frac{\varepsilon_2}{2} \tag{6}$$

By removing ε_1 and ε_2 from equations (2), (3), (4), (5) and (6), we obtain the error on differential current level 2, as a function of the measured average current and the previous current level 2, as shown in (7):

$$\varepsilon_2 = \frac{3\mu_m}{\frac{n_{c1}}{2} + n_{c2}} - I_2[s-1] \tag{7}$$

A similar approach is used to extract ε_1:

$$\varepsilon_1 = \frac{3\mu_m}{n_{c1} + 2n_{c2}} - I_1[s-1] \tag{8}$$

With the errors on both current levels, the new current levels can be updated. A conservative approach is used, to avoid that any wrongly recognized symbol by the correlation mechanism would sharply impact the current level estimations. For this purpose, a first order Infinite Impulse Response (IIR) is used to filter the updated current, as shown in (9) and (10), where α is a positive real much smaller than 1. The smaller α, the more conservatively the currents are updated, with a negative impact on the convergence to the optimal currents.

$$I_1[s] = I_1[s-1](1-\alpha) + a(I_1[s-1] + \varepsilon_1) = I_1[s-1] + \alpha\varepsilon_1 \tag{9}$$

$$I_2[s] = I_2[s-1] + \alpha\varepsilon_2 \tag{10}$$

The thresholds after sample s was received, $T_{01}[s]$ and $T_{12}[s]$, between current levels 0 and 1 and current levels 1 and 2, respectively, are the middle values between the current levels, as shown in (11) and (12):

$$T_{01}[s] = \frac{I_1[s]}{2} \tag{11}$$

$$T_{12}[s] = I_1[s] + \frac{I_2[s] - I_1[s]}{2} = \frac{I_1[s] + I_2[s]}{2} \tag{12}$$

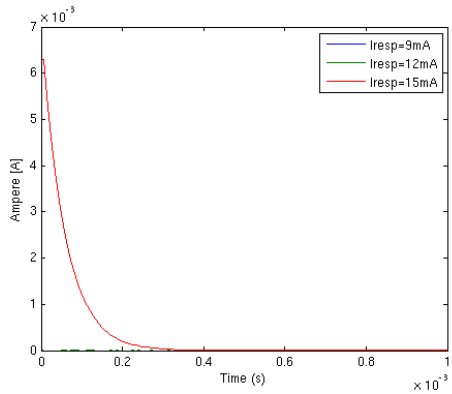

Figure 3. Δ_{12} extreme current deviations.

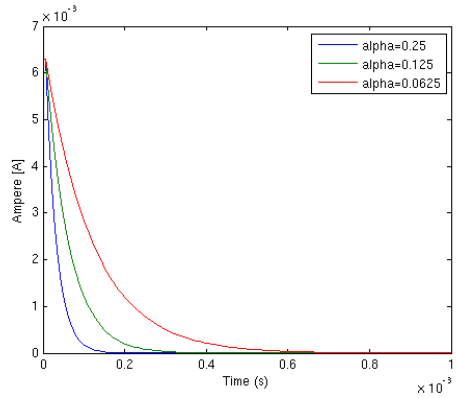

Figure 4. Influence of α on Δ_{12}.

V. Performance Estimation

The nominal value of I_{RESP} is defined in [1] to be 12mA, therefore, the nominal value of T_{12} is 18mA. In reference [1], the sensors are allowed to deviate by 12.5% from the nominal value. The combined line attenuation and the receiver gain error also create a deviation from the nominal value of another 20%. The total error from sensor current modulation to the input to the quantizer can reach overall +35% to -30%. We then have that the expected threshold between levels 0 and 1, $E_{01}[s]$, can have any value between $0.35I_{RESP}$ and $0.675I_{RESP}$. The expected threshold between levels 1 and 2, $E_{12}[s]$, can have any value between $1.05I_{RESP}$ and $2.025I_{RESP}$.

The performance can be measured by introducing the difference between the expected threshold, $E_{12}[s]$ and $T_{12}[s]$, $\Delta_{12}[s]$, for every sample:

$$\Delta_{12}[s] = |T_{12}[s] - E_{12}[s]| \tag{13}$$

The first simulations were run in a simplified system: there is no signal distortion between the sensor and the master, no quiescent current and the correlation mechanism always recognizes the correct symbol. In Fig. 3, the current level I_{RESP} was set to the extreme values and the nominal value, with $\alpha=2^{-3}$. For the extreme

current levels, we see a transient behavior until there is convergence to zero error. The nominal I_{RESP} stays always without error. The positive and negative extreme I_{RESP} currents have an identical behavior. In Fig. 4, we use I_{RESP} 35% below the nominal value, and modify α. A bigger α reduces the settling time to the zero error.

The threshold adaptation algorithm is used in conjunction with the rest of the system depicted in Fig. 2. The following simulations were run with the complete system including the sensor, transmitting modulated current, harness, voltage regulation and bit decoding modeled in SimuLink. Four load models were defined, at the expected worst system response. The load models include the sensor serial capacitor, C_s, serial resistor, R_s, the harness capacitor, C_e, and its parasitic serial inductance, L_e. The values used for each load model are summarized in Table II. All test cases have 12 frames of 32 bits each and t_{chip}=2.5 µs.

TABLE II. VALUES OF PARAMETERS FOR ALL SHOWN RESULTS

Load model index	5	8	9	12
C_s(nF)	40	20	10	5
C_e(nF)	35	35	5	5
R_s(Ω)	0.6	1.2	2.5	2.5
L_e(µH)	1.2	1.2	1.2	1.2

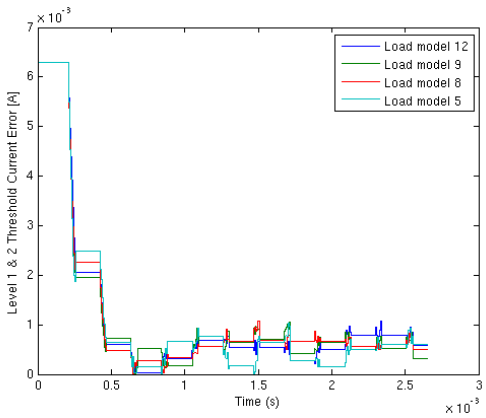

Figure 5. Δ_{12} for considered load models.

All load models defined above were simulated with 35% positive error and $\alpha=2^{-3}$. The results are shown in Fig. 5. The variation around the converging threshold current has two causes of error:

- The capacitive load. As can be seen from Table I, not all symbols have the same amount of level transitions from high to low as from low to high level. This effect causes either an over estimation of μ_m (for example for data 4, if the last chip of the previous symbol has level 2) or an under estimation of μ_m (for example for data 6, if the last chip of the previous symbol has level 0).
- The Correlation mechanism. The pattern recognition is based on checking correlation score between the incoming symbol and all possible expected patterns. Once a high score for one of the expected patterns was reached, the symbol is recognized. Depending on how the load distorted the current, the correlation mechanism will take a varying amount of samples to recognize the pattern. Therefore, the symbol boundaries may include samples from the previous symbol, causing a wrong estimation of μ_m.

More simulations were run with varying α on load model 4, with 35% positive error. The results are shown on Fig. 6. As was shown with the ideal case, the convergence speed increases with α. The advantage of keeping a lower α is to have less sensitivity to the load model. The variation due to incorrect current estimation on a single symbol is reduced with a small α.

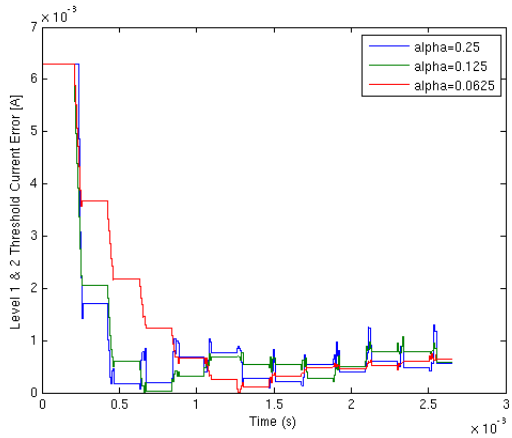

Figure 6. Δ_{12} with varying α on a typical load model.

VI. CONCLUSION

This paper proposed a way to estimate and adapt the thresholds used by a quantizer for DSI3 sensor to master symbol detection. We listed existing quantization level adaptation methods. We analytically detailed our method for quantization levels based on the feedback of the correlation mechanism. The performance was analyzed both in a simplified environment and a realistic complete system. The results show a steady state error which is below 6% from an initial 35% error and a convergence to this error range within 24 symbols when the system includes all current distortions and the correlation mechanism inaccuracies.

REFERENCES

[1] Distributed System Interface 3 Bus Standard Revision 1.00, DSI3 Consortium, February 11, 2011.

[2] Peripheral Sensor Interface for Automotive Applications, PSI5 Steering Committee, Version 2.0, June 1st, 2011.

[3] N. S. Jayant, "Adaptive quantization with a one-word memory," *The Bell System Technical Journal*, vol. 52, no. 7, September, 1973.

[4] R. Kwok and W. T. K. Johnson, "Block adaptive quantization of magellan SAR data," *IEEE Transactions on Geoscience and Remote Sensing*, vol. 27, no. 4, July 1989.

[5] Z. Peric, J. Nikolic, A. Mosic, and S. Panic, "A switched-adaptive quantization technique using µ-law quantizers," *Information Technology and Control*, vol. 9, no. 4, pp. 317–320, August 2010.

[6] A. Ortega and M. Vetterli, "Adaptive scalar quantization without side information," *IEEE Transactions on Image Processing*, vol. 6, no. 5, pp. 665-676, May 1997.

[7] M. Mansouri, I. Ouachani, H. Snoussi, and C. Richard, "Cramer-rao bound-based adaptive quantization for target tracking in wireless sensor networks," in *Proc. IEEE Workshop on Statistical Signal Processing*, September 2009, pp. 693-696.

[8] D. G. Jeong and J. D. Gibson, "Image coding with uniform and piecewise uniform vector quantizers," in *Proc. Global Telecommunications Conference*, vol. 1, 2-5 December 1991, pp. 80-84.

[9] A. P. Dempster, N. M. Laird, and D. B. Rubin, "Maximum likelihood from incomplete data via the EM algorithm," *Journal of the Royal Statistical Society, Series B (Methodological)*, vol. 39, no. 1, pp. 1-38, 1977.

David Levy was born in Sarcelles, France on March 7, 1970. Levy graduated in Electronics in 1993 with honors at Université Libre de Bruxelles, Belgium, focusing on computer networks. Levy has several patents and a publication related to WLAN in particular and telecommunication in general. He worked in several startup companies as a Board and Digital Designer until 2000. He was the System Architect of the MAC layer for an ADSL modem at Alcatel and STMicroelectronics from 2000 to 2005. He was the WLAN System Architect at Texas Instruments, working on the complete WLAN transceiver in a chip for mobile phones from 2006 to 2009. Since 2010, he is a Concept Engineer for Automotive Airbag SoC at Infineon, Villach in Austria, focusing on the sensor interface and the Embedded Safing Engine. From 2006 to 2009 Mr. Levy was an active member of the Wi-Fi Alliance.